Interpreting CMS data in the phenomenological MSSM

Maurizio Pierini

CERN

Maria Spiropulu

CERN & California Institute Of Technology, Pasadena

Filip Moortgat, Luc Pape

ETH, Zurich, Switzerland

Joseph Lykken

Fermi National Accelerator Laboratory, Batavia, Illinois

Harrison Prosper, Sezen Sekmen

Florida State University, Tallahassee

Sabine Kraml

LPSC Grenoble, France

Sanjay Padhi

University of California, San Diego

Abstract

We interpret the data taken with the CMS detector during the 7 TeV LHC run within the phenomenological MSSM (pMSSM). The pMSSM is a 19-dimensional parametrization of the general MSSM, that captures most of the phenomenological features of the MSSM. It encompasses, and goes beyond, a broad range of more constrained SUSY models (such as the CMSSM). Using profile likelihoods, we examine the influence of each of the 19 parameters and determine to which parameters (and derived observables) the current CMS data are most sensitive. We provide generic constraints on quantities sensitive to hadronic as well as multilepton final states, based on the 2010 CMS data-set corresponding to 35 pb^{-1} of integrated luminosity. In contrast to constraints derived for particular SUSY-breaking schemes such as the CMSSM, our results provide more generic conclusions on how the current data can constrain the MSSM. Moreover, while the focus of this note is the MSSM, the approach we describe is applicable to *any* multi-parameter model.

1 Introduction

After the successful operation of the Large Hadron Collider (LHC) and the CMS detector in 2010, and with good prospects for the future, the LHC is now ready to shed light on a number of open questions in Particle Physics, such as the mechanism of electroweak (EW) symmetry breaking, or the nature of new physics Beyond the Standard Model (BSM) needed to stabilize the EW scale.

A wealth of theories that extend the Standard Model has been put forth in the past decades. The arguably best motivated such BSM theory — and certainly the most thouroughly studied one — is supersymmetry (SUSY). Indeed, searches for SUSY are among the primary objectives of the CMS experiment. Note that SUSY is exceedingly popular not only for its theoretical beauty but also because SUSY phenomenology is extremely rich, leading to a large variety of possible new signals at the LHC. In spite of this, the majority of SUSY studies focusses on a very special setup: the so-called Constrained Minimal Supersymmetric Standard Model (CMSSM). This was justified in the preparation for discoveries as the CMSSM, having just a handful of new parameters, is very predicive. However, the simple assumption of universality at the GUT scale lacks a sound theoretical motivation; the CMSSM should hence be regarded as a showcase model. When it comes to interpreting experimental results, on the one hand it is reasonable and interesting to do this within the CMSSM, as it provides (to a certain extent) an easy way to show performances, compare limits or reaches, etc. On the other hand, the interpretation in the $(m_0, m_{1/2})$ plane risks to heavyly overconstrain SUSY, as many possible mass patterns and signatures are not covered in the CMSSM. The same problem actually arises in any analysis that assumes a particular SUSY breaking scheme.

In this Note we therefore introduce a different approach, which uses only minimal assumptions on the underlying SUSY parameters. In particular we do not rely on a particular SUSY breaking scheme. Instead, we use a 19-dimensional parametrization of the general MSSM, with parameters defined at the SUSY scale (by convention the geometric mean of the two stop masses), the so-called *phenomenological MSSM* (pMSSM). We here demonstrate the feasibility of our approach by applying it to the 2010 CMS data-set corresponding to 35 pb^{-1} of integrated luminosity. Using profile likelihoods, we combine the dijet α_T analysis, the opposite-sign dilepton analysis and the same-sign dilepton analysis and derive constraints on the SUSY particles that imply as few simplifying assumptions as possible. Results from other SUSY analyses in CMS will be added as soon as they become available.

In this Note, we first give the motivation to go beyond CMSSM and work in a generic MSSM setup. After this, the pMSSM and its parametrization is defined. We then outline our analysis, giving details on the pMSSM points we have used, the detector simulation and the CMS analyses, and describe the statistical method based on profile likelihoods used for coping with the 19-dimensional setup of our model. Finally, we discuss our results and summarize our conclusions.

2 Motivation for a generic MSSM setup

Perhaps the least understood aspect of SUSY is how its breaking can occur, which in turn determines the boundary conditions for the Lagrange parameters at some high scale. Theorists have postulated various possible scenarios, including supergravity (SUGRA), gauge mediation (GMSB), anomaly mediation (AMSB), gaugino mediation, radion mediation, etc.. They come in minimal (mSUGRA, mGMSB, ...) and less minimal (*e.g.*, non-universal Higgs masses, NUHM, or non-universal gaugino masses) variants, as well as in general setups (general gauge mediation, ...). Moreover, there are models of compressed, effective or split SUSY, GUT-inspired models, string-inspired models, and so on. Each of these possibilities features characteristic relations between fundamental parameters and hence characteristic mass spectra, decay patterns and properties of the dark matter candidate.

The CMSSM covers just a subset of this spectrum. To give some examples:

- The CMSSM assumes universal gaugino masses $M_1 = M_2 = M_3 \equiv m_{1/2}$ at the GUT scale, leading to

$$M_1 : M_2 : M_3 \approx 1 : 2 : 7 \text{ with } M_1 \approx 0.4\, m_{1/2} \tag{1}$$

  at the EW scale, which is equivalent to $m_{\tilde{\chi}^0_2} \approx 2m_{\tilde{\chi}^0_1} \approx 0.8\, m_{1/2}$ and $m_{\tilde{g}} \approx 7m_{\tilde{\chi}^0_1} \approx 2.8\, m_{1/2}$. Other models can have very different relations between M_1, M_2, M_3, giving rise to the so-called "gaugino code" [1], which can be very useful for model discrimination. Besides, models with non-universal gaugino masses are quite natural [2] even within the SUGRA context, and they can have very low finetuning [3].

- Over most of the CMSSM parameter space $|\mu|^2 \gtrsim m^2_{1/2}$. The lightest neutralino is then mostly bino, the second-lightest mostly wino, and the heavier ones mostly higgsinos. Light higgsinos and large gaugino–higgsino mixing (mixed bino–higgsino dark matter) occur only in the focus point region, *i.e.* when squarks

and sleptons are very heavy. This has a strong impact on squark and gluino cascade decays, as well as on the part of parameter space that is compatible with dark matter constraints.

- Turning to the sfermion sector, the slepton-mass parameters are to good approximation

$$m^2_{\tilde{E}} \approx m^2_0 + 0.15\, m^2_{1/2}\,, \qquad m^2_{\tilde{L}} \approx m^2_0 + 0.5\, m^2_{1/2}\,. \tag{2}$$

Note that this implies that right-chiral states are alway lighter than the left-chiral ones. Combining Eqs. (1) and (2) we see that for small m_0 (but large enough to have a neutralino LSP) this leads to the typical mass pattern $m_{\tilde{\chi}^0_1} < m_{\tilde{e}_R} < m_{\tilde{\chi}^0_2} < m_{\tilde{e}_L}$. For the first two generations of squarks we have

$$m^2_{\tilde{U},\tilde{D}} \approx m^2_0 + K m^2_{1/2}\,, \qquad m^2_{\tilde{Q}} \approx m^2_0 + (K+0.5) m^2_{1/2}\,, \tag{3}$$

with $K \sim 4.5$ to 6.5, and the dependence on $m_{1/2}$ dominated by the gluino contribution, *i.e.* by M_3. It is clear that any limit on or determination of m_0 is completely dominated by the slepton sector [4]. Non-universal scalar masses are heavily constrained by flavour-changing neutral currents (FCNC), at least for the first and second generations. For the third generation, the FCNC constraints are much less severe. One possibility to motivate universal mass parameters for sfermions is to embed them in a higher gauge group, like SO(10). But even then, non-universalities can occur through D-term contributions [5] and/or GUT-scale threshold corrections [6, 7]. Besides, there is no sound theoretical motivation for unifying the mass-squared terms of the Higgs fields, $m^2_{H_1}$ and $m^2_{H_2}$, with those of the other scalars. If this is given up $m^2_{H_{1,2}}$, or equivalently μ and m_A, become free parameters of the model [8] (cf. the discussion of the value of μ above).

- The assumption of scalar mass universality has another important implication, namely that the renormalization-group invariant quantity

$$S = \left(m^2_{H_2} - m^2_{H_1}\right) + \mathrm{Tr}\left(m^2_{\tilde{Q}} - 2m^2_{\tilde{U}} + m^2_{\tilde{D}} + m^2_{\tilde{E}} - m^2_{\tilde{L}}\right) \tag{4}$$

vanishes. This so-called S-parameter, if non-zero, influences the running of the scalar mass parametres m^2_ϕ proportional to their hypercharge Y_ϕ

$$16\pi^2 \frac{d}{dt} m^2_\phi = ... + \frac{6}{5} Y_\phi g_1^2 S\,. \tag{5}$$

This can change the mass ordering of left- and right-chiral states or have an important influence on the Higgs sector. In the CMSSM however $S \equiv 0$.

From these considerations, which are just exemplary and by no means complete, it is clear that it is interesting and necessary to go beyond the naïve CMSSM. Our approach should be to search for SUSY without prejudice [9, 10], even more so since we have the necessary knowledge and machinery at our disposal. In this context note that major efforts have recently been devoted to developing precise statistical tools for analyzing new physics at the LHC [11]. This includes sophisticated methods and tools for the investigation of multi-dimensional parameter spaces, as typical for SUSY models. Below we therefore lay out a program for the investigation of the phenomenological MSSM, which gets by with only a minimal set of assumptions. Most importantly it allows us to cover the full range of possible mass patterns and of neutralino dark matter properties.

3 Phenomenological MSSM (pMSSM)

As mentioned, the pMSSM is a 19-dimensional realization of the MSSM with parameters defined at the so-called SUSY scale[1)] $M_{\rm SUSY} = \sqrt{m_{\tilde{t}_1} m_{\tilde{t}_2}}$. We first explain this number of parameters and their implications?

In its most generic form, just assuming R-parity conservation, the MSSM has over 120 free parameters: SUSY-breaking mass terms and trilinear couplings, Yukawa matrices, CP phases, two VEVs, and a superpotential μ term. Model builders construct theoretically-motivated economic models that provide relations between these parameters at some high scale, *e.g.*, the GUT scale. These then evolved to $M_{\rm SUSY}$ by renormalization group equations to derive model-specific testable predictions. On the other hand, it is expected that once SUSY particles are discovered, measurements of their masses and interactions will allow to reconstruct (at least part of) the Lagrange parameters and thus infer the underlying SUSY breaking mechanism.

[1)] Sometimes also referred to as the scale of electroweak symmetry breaking, $M_{\rm EWSB}$.

Luckily not all of the ∼120 MSSM parameters are of equal relevance to this end. In fact, a couple of reasonable assumptions motivated by experiment serve to simplify the problem a lot. In particular, it is reasonable to restrict ourselves to the CP-conserving MSSM (*i.e.* no new CP phases) with minimal flavor violation (MFV). Constraints from the flavor sector moreover suggest that the first two generations of sfermions be taken to be degenerate. Regarding Yukawa and trilinear couplings, only those of the third generation matter at leading order. Finally, we assume that the gravitino is heavy[2)] and the lightest supersymmetric particle (LSP) is the lightest neutralino, $\tilde{\chi}_1^0$.

This leaves us with the 19 real, weak-scale SUSY Lagrange parameters that define the pMSSM:

- 3 gaugino masses M_1, M_2, and M_3 (pertaining to U(1), SU(2), and SU(3) gauginos, respectively);
- the higgsino mass parameter μ;
- the ratio of the Higgs VEVs $\tan\beta = v_2/v_1$;
- the pseudo-scalar Higgs mass m_A;[3)]
- 10 sfermion mass parameters $m_{\tilde{F}}$, where $\tilde{F} = \tilde{Q}_1, \tilde{U}_1, \tilde{D}_1, \tilde{L}_1, \tilde{E}_1, \tilde{Q}_3, \tilde{U}_3, \tilde{D}_3, \tilde{L}_3$, and $\tilde{E}_3$ (recall that $m_{\tilde{Q}_1} \equiv m_{\tilde{Q}_2}$, $m_{\tilde{L}_1} \equiv m_{\tilde{L}_2}$, etc.); and
- 3 trilinear couplings A_t, A_b and A_τ

In [9], Berger *et al.* performed a scan of the pMSSM parameters to find out what regions of parameter space are consistent with theoretical and experimental constrains. In particular they did a uniform random sampling of points from within the following ranges:[4)]

$$\begin{aligned} 100\text{ GeV} \leq\ & m_{\tilde{F}} && \leq 1000\text{ GeV}, \\ 50\text{ GeV} \leq\ & |M_{1,2}, \mu| && \leq 1000\text{ GeV}, \\ 100\text{ GeV} \leq\ & M_3 && \leq 1000\text{ GeV}, \\ & |A_{t,b,\tau}| && \leq 1000\text{ GeV}, \\ 1 \leq\ & \tan\beta && \leq 50, \\ 43.5\text{ GeV} \leq\ & m_A && \leq 1000\text{ GeV}, \end{aligned} \tag{6}$$

Imposing SUSY and Higgs mass limits and requiring consistency with low-energy constraints and with the dark matter relic density, they found [9] that *"the pMSSM leads to a much broader set of predictions for the properties of the SUSY partners as well as for a number of experimental observables than those found in any of the conventional SUSY breaking scenarios such as mSUGRA [CMSSM]. This set of models can easily lead to atypical expectations for SUSY signals at the LHC."*

As a first step towards a full pMSSM analysis, we use a 6K subset of the pMSSM points generated by Berger *et al.* and investigate to which extent CMS SUSY analyses with 35 pb^{-1} of data already constrain this sample.

4 Analysis

The goal of this study is to determine whether current CMS data are sufficient to impose visible constraints on the pMSSM parameter space, and consequently on SUSY mass scales and low energy observables such as $(g-2)_\mu$, BR($b \to s\gamma$), etc. To achieve this goal, we carry out the following analysis steps:

- For each of the 6K pMSSM points we generate 10K events.
- We perform three approved CMS analyses, namely the "di-jet α_T" (Had), "opposite-sign di-lepton" (OS) and "same-sign di-lepton" (SS) analyses on each of the 6K pMSSM samples.

[2)] To be completely honest, this implies after all some assumption on the SUSY breaking mechanism; for instance it excludes low-scale gauge mediation.

[3)] The parameters μ and m_A can be swapped for the Higgs mass parameters $m_{H_1}^2$ and $m_{H_2}^2$.

[4)] Here note that M_1, M_2, μ, A_t, A_b and A_τ can have arbitrary signs; M_3 was chosen to be positive because only six of all possible sign combinations of M_i, A_i, μ are physical.

- For each pMSSM point and for each of the three analyses, we combine the predicted signal yield s with the approved CMS results—the observed event count N and a data-driven background estimate $b \pm \delta b$—to compute the likelihood as a function of the pMSSM parameters.
- We weight every pMSSM point with the product of the three likelihoods, one for each of the three analyses. Since the pMSSM points were sampled from a (bounded) uniform 19-dimensional density, the set of weights constitute a non-parametric representation of the likelihood function.
- In order to illustrate the contribution of the current CMS data, we calculate profile likelihoods for the relevant model parameters, with and without the CMS likelihood, that is, the weights.

4.1 Event samples

We use a 6K subset of the pMSSM points generated by Berger *et al.* as explained in Section 3. Information on each point is contained in a SUSY Les Houches (SLHA) [23] file. For each point, 10K events were generated using `PYTHIA6` [24]. We simulate the response of the CMS detector using the publicly available general purpose detector simulation package `Delphes` [25]. Through extensive numerical and shape comparisons we conclude that we are able to provide a *very* fast simulation of the CMS detector that is good to within 10%. An accurate, fast, simulation is critical for studies of this scope.

4.2 Implementation of the three approved CMS analyses

The hadronic as well as multileptons analyses are performed on the simulated and reconstruction events. The hadronic analysis agrees with the full simulation results within 10%. Details on comparison between the reconstructed quantities can be found in the Section 6. For the leptonic studies the agreement is within 25%, during the next iteration we plan to use the efficiency model as outlined in [30].

The following table shows the Numerical results of the three CMS analyses for 35 pb^{-1} of luminosity.

Table 1: Numerical results of the three CMS analyses for 35 pb^{-1} as given by `CMSSW` full simulation and `Delphes` for the SUSY benchmarks LM0 and LM1.

Analysis (k)	Observed data count (N_k)	Data-driven SM BG estimate ($b_k \pm \delta b_k$)	MC SM BG prediction ($b_k^{MC} \pm b_k^{MC}$)
Dijet α_T	14	11.4 ± 2.0	9.2 ± 0.9
OS di-lepton	1	2.1 ± 2.1	1.27
SS di-lepton	0	1.2 ± 0.8	0.35

4.3 Calculation of the likelihood function

Every analysis k yields an observed count N_k and a background estimate $b_k \pm \delta b_k$ where $k = 1, 2, 3$. We make the standard assumption that the counts are Poisson distributed in which case the total likelihood from the combination of the three analyses can be written as

$$L(\theta) \equiv p(N|s,b) = \prod_{k=1}^{3} \text{Poisson}(N_k|s_k + b_k), \tag{7}$$

where s_k is the predicted signal and $L(\theta)$ the likelihood written as a function of the d =19-dimensional pMSSM parameter θ. In this study, the map of θ to the expected signals s_k is represented non-parametrically using the 6K pMSSM points. In principle, we could build a smooth functional approximation to this map; however, we have not attempted this in the current study. The likelihood values $L(\theta_i)$, where i is the ith pMSSM point, is used as the weight for this point. This is how we incorporate the likelihood function of the three approved CMS analyses in our pMSSM interpretation of the CMS results.

For any likelihood function, exact confidence regions [29] can *always* be created in the unrestricted parameter space. However, such confidence regions are seldom useful when the dimensionality of the parameter space is large. It is more useful to examine parameters one or two at a time. In the current study, we examine each parameter separately using the profile likelihood, a broadly applicable frequentist construct.

4.4 Calculation of profile likelihoods

As noted above, an important goal of this study is to determine to which pMSSM parameters the current CMS dataset is most sensitive and to what degree. This is useful because we shall be able to make statements whose validity is much broader than those made using models in which strong, but weakly motivated, simplifying assumptions have been made. A well-established way of conveying relevant information about the parameters of interest is to display their 1-dimensional profile likelihoods. We do this for each pMSSM parameter as well as for some observables.

Suppose we wish to investigate the gluino mass parameter M_3. Its (1-dimensional) profile likelihood, L_p, [29] is defined by

$$L_p(M_3) \equiv L(M_3, \hat{\theta}_2(M_3), \cdots, \hat{\theta}_{19}(M_3)), \tag{8}$$

where $\hat{\theta}_2 \cdots \hat{\theta}_{19}$ denote the maximum likelihood estimates (MLE), for a given value of M_3, of the remaining 18 parameters. Since we do not have a functional approximation of the map from θ to the expected signals, our likelihood function $L(\theta)$ is available non-parametrically as a swarm of weighted points, so standard maximizing programs such as `MINUIT` cannot be used. We have therefore devised our own non-parametric profiling algorithm, which proceeds as follows:

1. For each 1-dimensional bin of the parameter or observable of interest, for example M_3, we create a d-dimensional histogram of the 6K points using the Root class `TKDTreeBinning`. Through recursive binary partitioning, this class creates d-dimensional bins with equal bin content.

2. For a given bin, e.g. in the gluino mass parameter M_3, we find which of the 6K points is consistent with the given value of M_3.

3. Using these points, we find the bin with the maximum density (the one with the smallest volume) and use that as an estimate of the profile likelihood value for the given value of M_3.

4. In addition, in order to provide a better estimate, the above procedure is repeated 100 times, each with a different bootstrap sample of the original 6K points and the average is taken over the profiles in each bin. This in turn is done for each of the ~ 70 variables under investigation.

5 Results

We present the results obtained by following the analysis path in Section **??**, in terms of plots of likelihood ratios L_p/L_{max} as a function of each parameter of interest. Further details on this ratio as a measure can be found in the Appendix.

Plots of the likelihood ratio L_p/L_{max} are shown for the 19 input pMSSM parameters in Figures 1 to 5. Similarly Figures 6 to 11 show the likelihood ratio for the physical sparticle masses. The relations between the scalar SUSY breaking mass parameters with the physical scalar masses as well as the gaugino mass parameters with the physical gaugino masses should be noted. The colored and shaded histograms in each plot depict the likelihood ratio before and after the inclusion of CMS results, respectively. We observe that the CMS results indeed introduce a variation in the likelihood ratios, where the variation is more enhanced for some parameters/masses and milder for others.

We see that all squark/slepton mass parameters and all squark/slepton masses shift upwards systematically after the addition of CMS results. The gaugino mass parameter M_3 and the gluino mass also move up simultaneously due to the constrains coming from the di-jet α_T analysis. An important aspect to note is that no significant change is observed in the distribution for the mass of $\tilde{\chi}_1^0$, which is the lightest supersymmetric particle (LSP), since neither a stringent E_{miss}^T cut nor any other technique dedicated to constraining the $\tilde{\chi}_1^0$ mass were imposed in the analyses considered. We owe our ability to observe this effect to the freedom offered by the pMSSM parameterization, in which neutralino/chargino masses are allowed to vary independently from the gluino mass. Had the interpretation been done using CMSSM, we would be influenced by the strict gaugino mass relationship described in Section 2, and the $\tilde{\chi}_1^0$ mass would be forced to move upwards in correlation along with the gluino mass.

Figure 12 shows L_p/L_{max} for the dark matter relic density calculated using `micrOMEGAs 2.4` [26] assuming $\tilde{\chi}_1^0$ is the LSP and the dark matter candidate. It must be noted that Berger *et al.* imposed the WMAP upper limit $\Omega_{\tilde{\chi}_1^0} h^2 \leq 0.1210$ as a constraint on the points. Information from CMS does modify the distribution, however the effect is not sufficient to impose a concrete constraint on $\Omega_{\tilde{\chi}_1^0} h^2$. This is of course related to the result on χ_1^0 mass.

Finally Figures 13 and 14 show distributions for low energy observables as predicted by pMSSM, calculated by `micrOMEGAs 2.4` and `Superiso 2.7` [27]. We again note that the constraints based on experimental measurements for a subset of these observables were taken into account while selecting the pMSSM points by Berger *et al.*. Similar to the case for the relic density, the 2010 CMS measurements do not yet allow us to constrain these observables further. However, the prospect of making statements on the predictions for low energy observables in the presence of more data and diverse analysis channels stands out as a strong motivation in favor of interpreting the data within the framework of supersymmetry.

The results we have presented here, with only 35 pb^{-1} of CMS data, show that even with modest amount of data, we are able to start making inferences of a general nature about supersymmetry. Therefore we anticipate that at least with an order of magnitude more data, the approach we have developed will allow us to make definitive statements about a broad class of supersymmetric models. This is only the starting point that has opened up a vast amount of investigation. We will develop this study further by considering the following:

- An improved treatment of the constraints from the EW observables. We shall replace the box-like likelihood of Berger *et al* by a well-defined likelihood function.
- A significant increase in the sample of pMSSM points
- Inclusion of a wider range of final states
- The construction of a more quantitative treatment of the bounds on the pMSSM parameter space.

6 Conclusion

We presented the first interpretation of 35 pb^{-1} CMS data collected in 2010 within the framework of phenomenological MSSM, which is a sufficiently generic and well-motivated 19-dimensional parameterization of SUSY defined at the SUSY scale. We have used three well-developed CMS SUSY analyses, namely, di-jet α_T, opposite-sign dilepton and same-sign di-lepton for this purpose, and expressed our results in terms of likelihood ratios. We have demonstrated that interpretation of CMS data in terms of broad classes of multi-parameter SUSY models is feasible with the currently available statistical tools, and that it is indeed possible to make meaningful statements on the natures of such models.

Acknowledgements

We thank JoAnne Hewett and Thomas G. Rizzo for providing us the 6K pMSSM points used in this analysis.

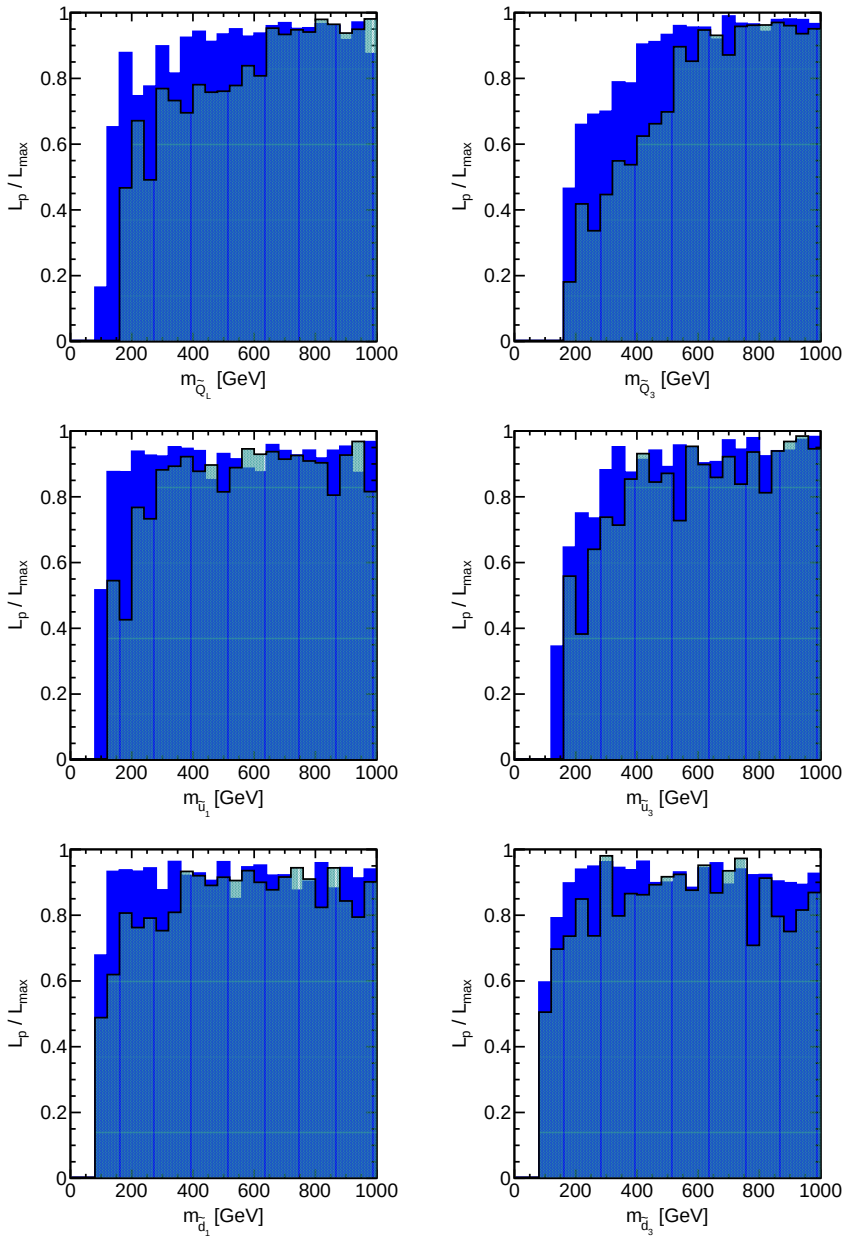

Figure 1: Ratios of profile likelihood L_p to maximum likelihood L_{max} shown for the squark mass parameters at SUSY scale. The colored and shaded histograms show the distributions before and after the inclusion of the CMS results.

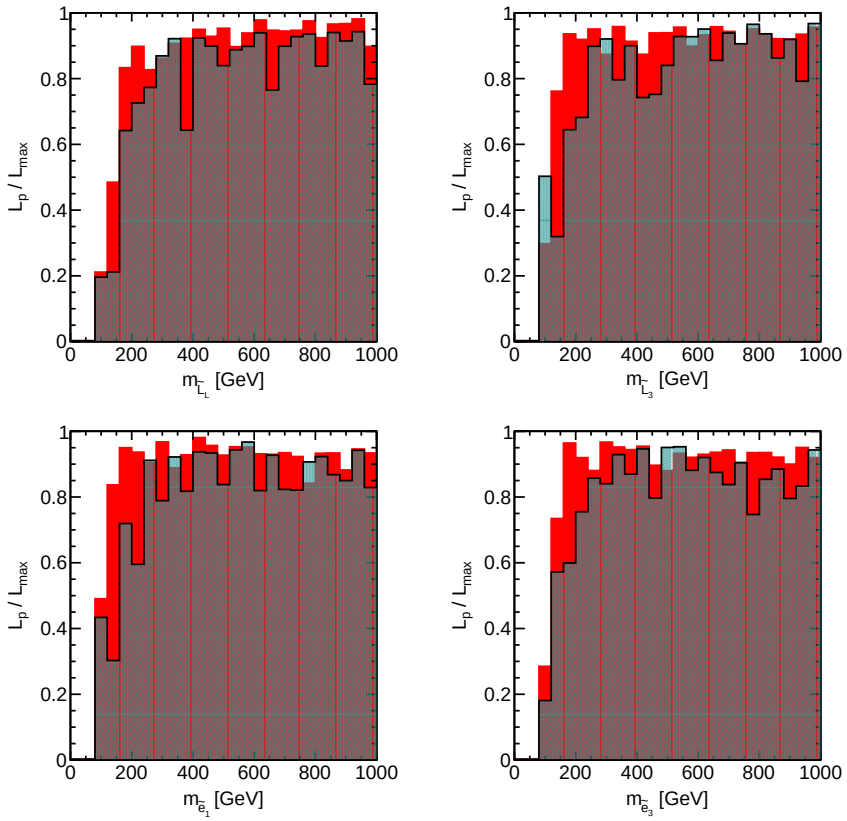

Figure 2: Ratios of profile likelihood L_p to maximum likelihood L_{max} shown for the slepton mass parameters at SUSY scale. The colored and shaded histograms show the distributions before and after the inclusion of the CMS results.

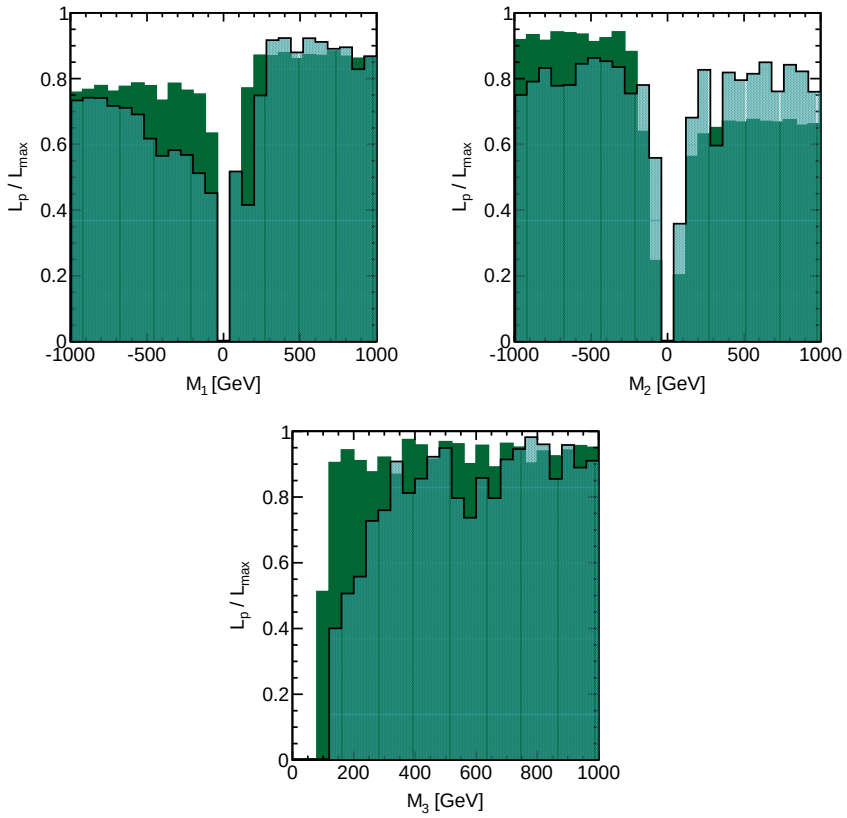

Figure 3: Ratios of profile likelihood L_p to maximum likelihood L_{max} shown for gaugino mass parameters at SUSY scale. The colored and shaded histograms show the distributions before and after the inclusion of the CMS results.

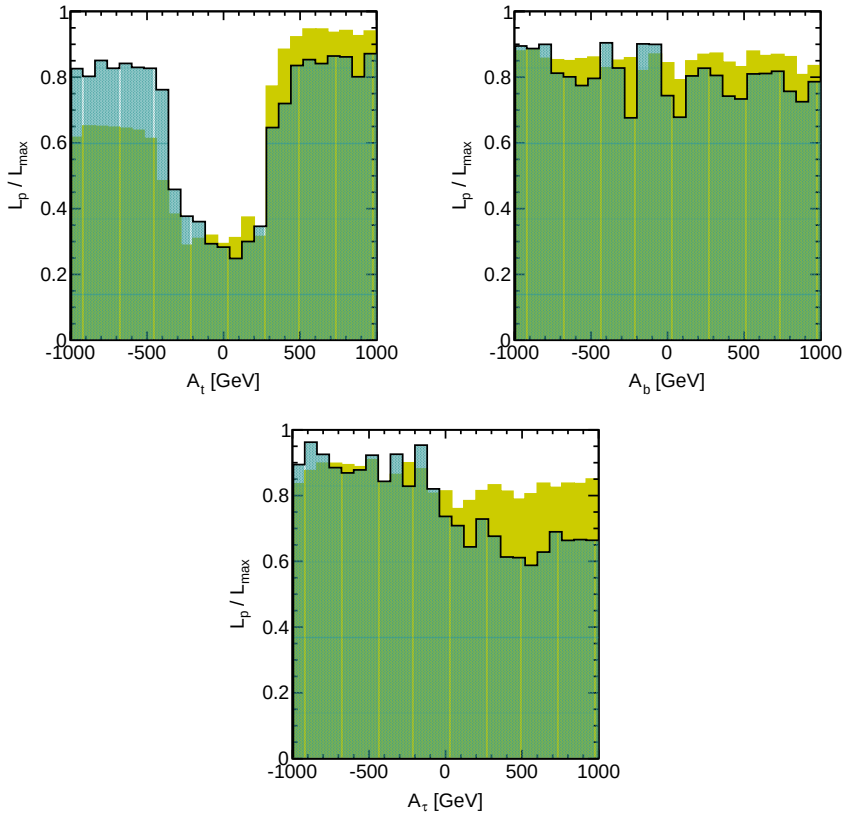

Figure 4: Ratios of profile likelihood L_p to maximum likelihood L_{max} shown for trilinear couplings at SUSY scale. The colored and shaded histograms show the distributions before and after the inclusion of the CMS results.

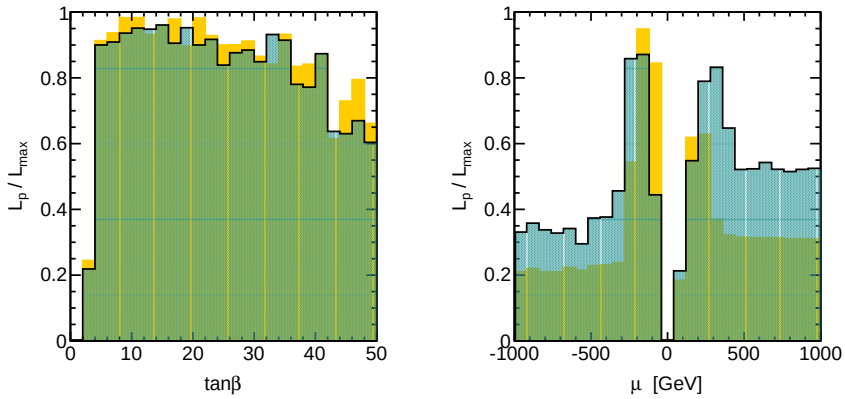

Figure 5: Ratios of profile likelihood L_p to maximum likelihood L_{max} shown for $\tan\beta$ and μ parameter at SUSY scale. The colored and shaded histograms show the distributions before and after the inclusion of the CMS results.

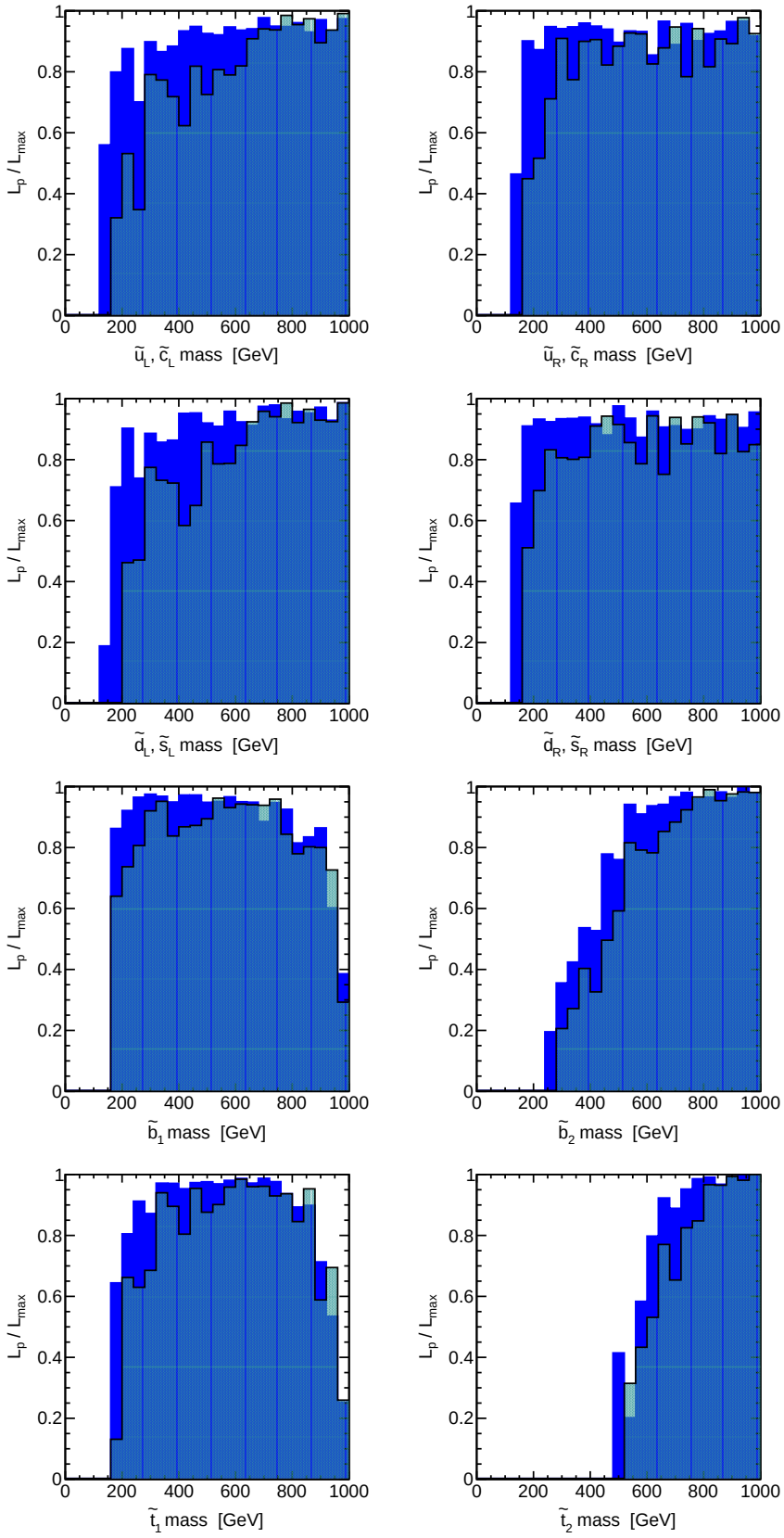

Figure 6: Ratios of profile likelihood L_p to maximum likelihood L_{max} shown for squark masses. The colored and shaded histograms show the distributions before and after the inclusion of the CMS results.

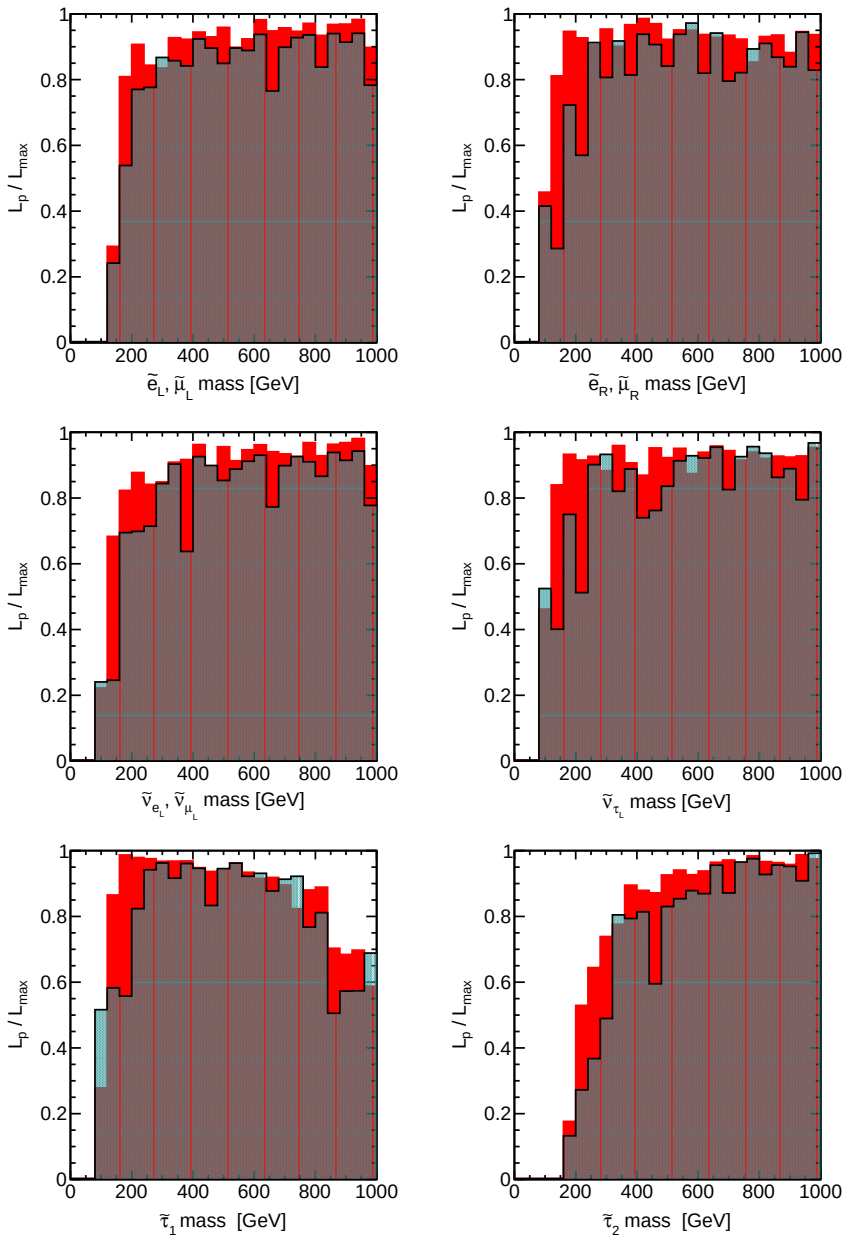

Figure 7: Ratios of profile likelihood L_p to maximum likelihood L_{max} shown for predictions for slepton masses. The colored and shaded histograms show the distributions before and after the inclusion of the CMS results.

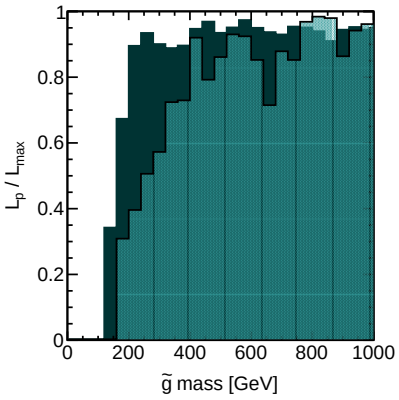

Figure 8: Ratios of profile likelihood L_p to maximum likelihood L_{max} shown for the gluino mass. The colored and shaded histograms show the distributions before and after the inclusion of the CMS results.

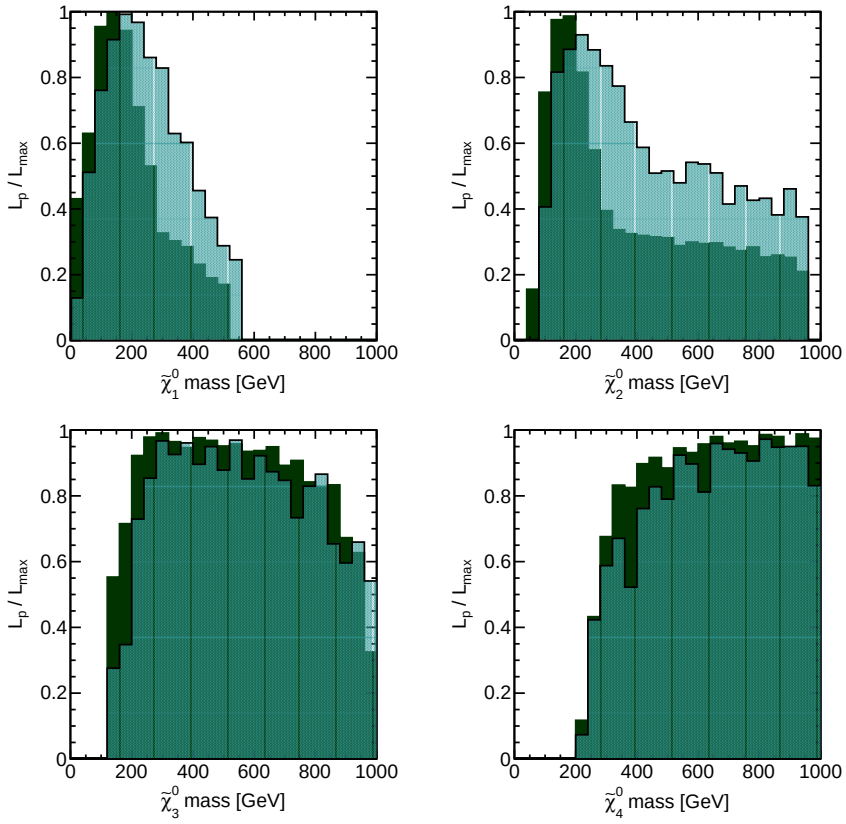

Figure 9: Ratios of profile likelihood L_p to maximum likelihood L_{max} shown for the neutralino masses. The colored and shaded histograms show the distributions before and after the inclusion of the CMS results.

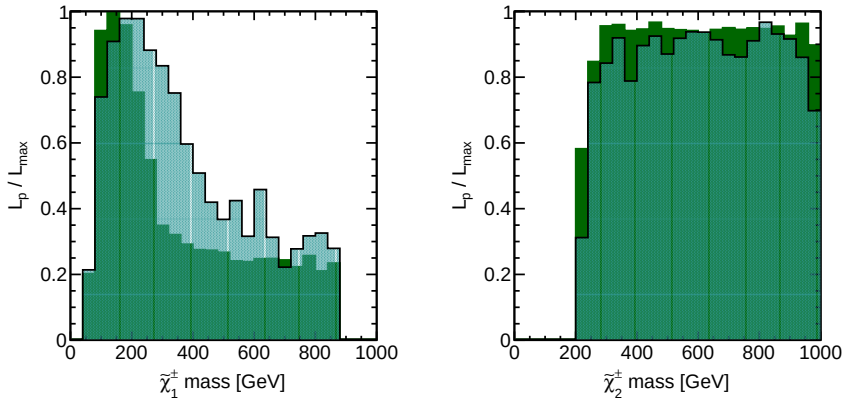

Figure 10: Ratios of profile likelihood L_p to maximum likelihood L_{max} shown for chargino masses. The colored and shaded histograms show the distributions before and after the inclusion of the CMS results.

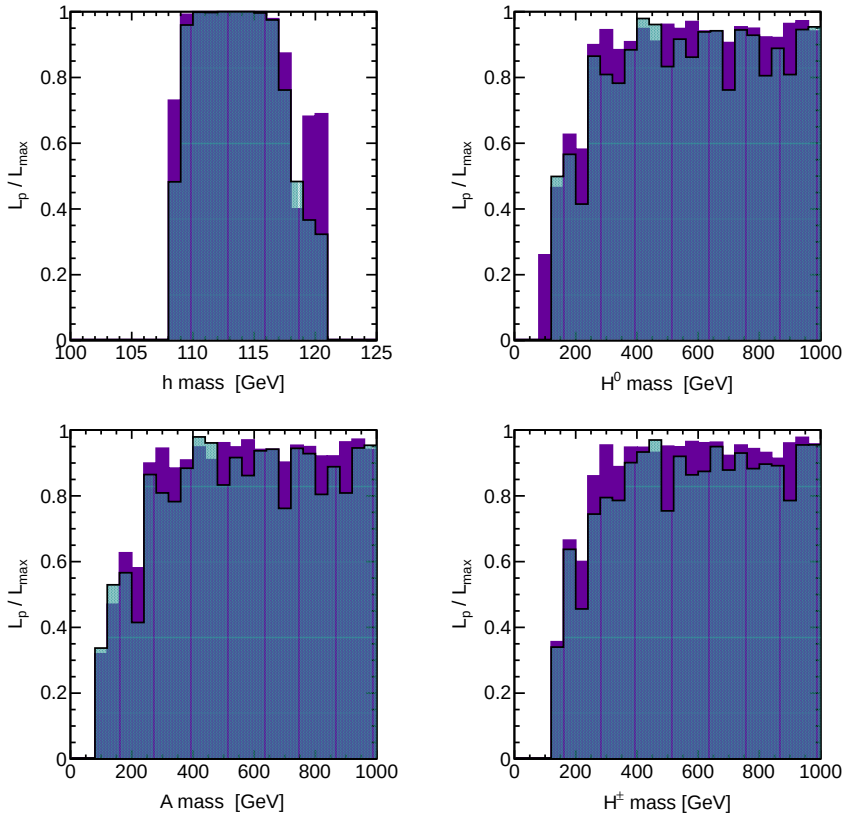

Figure 11: Ratios of profile likelihood L_p to maximum likelihood L_{max} shown for the Higgs masses. The colored and shaded histograms show the distributions before and after the inclusion of the CMS results.

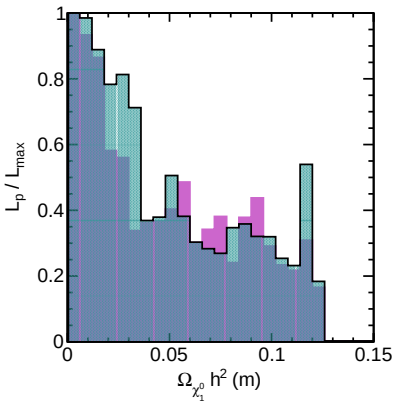

Figure 12: Ratio of profile likelihood L_p to maximum likelihood L_{max} shown for lightest neutralino dark matter relic density. The colored and shaded histograms show the distributions before and after the inclusion of the CMS results.

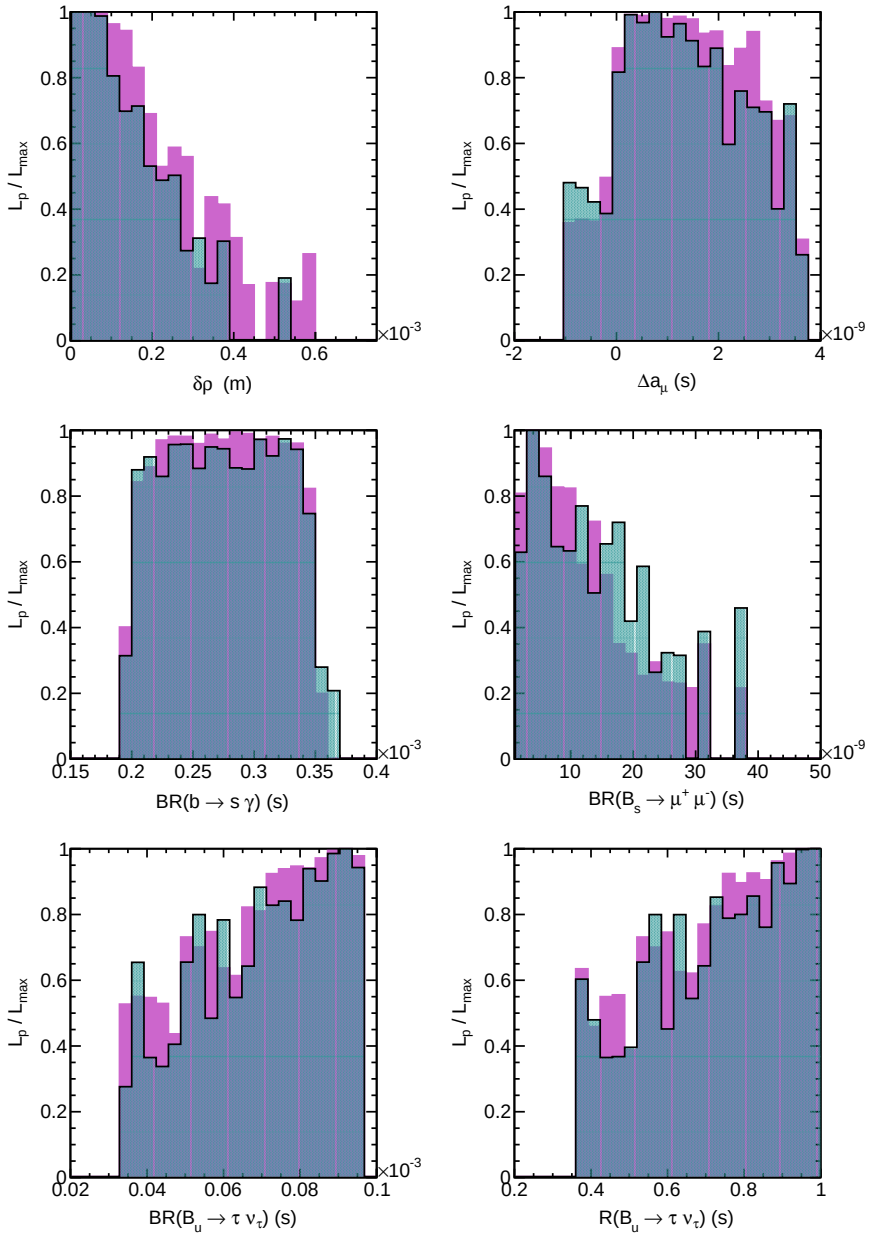

Figure 13: Ratios of profile likelihood L_p to maximum likelihood L_{max} shown for predictions for weak scale observables. $\delta\rho$ is calculated using `micrOMEGAs 2.4` and the rest are calculated using `Superiso 2.7`. The colored and shaded histograms show the distributions before and after the inclusion of the CMS results.

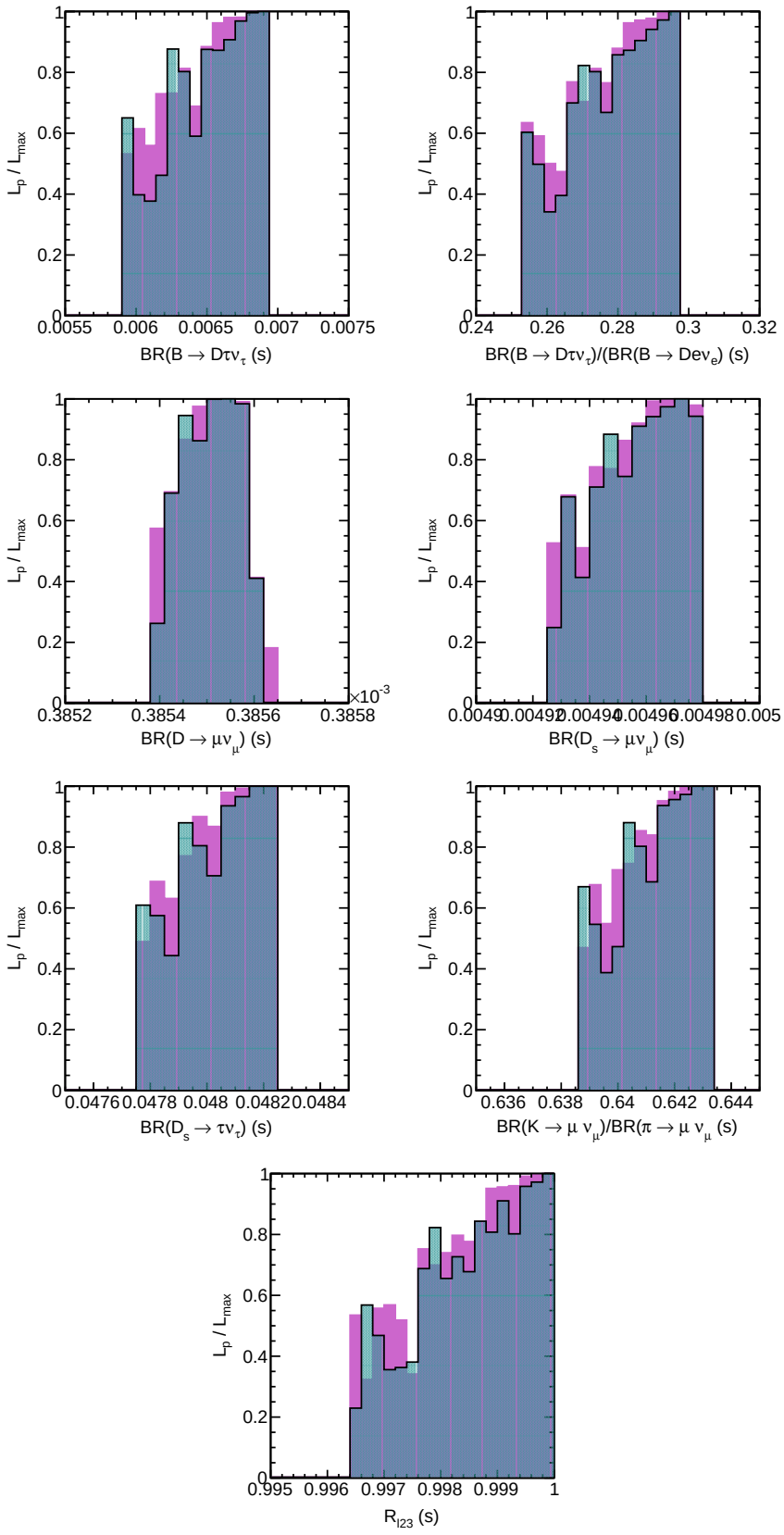

Figure 14: Ratios of profile likelihood L_p to maximum likelihood L_{max} shown for predictions for weak scale observables as calculated by `Superiso 2.7`. The colored and shaded histograms show the distributions before and after the inclusion of the CMS results.

Appendix

We describe the (frequentist) statistical procedures we have used in this study. Suppose that our goal is to make a statement about the parameter θ_1, say the gluino mass parameter M_3, independently of the remaining 18 pMSSM parameters. Since the expected signal s is a function of $d = 19$ parameters (see Sect. (**??**), which we denote by $\theta = \theta_1, \cdots, \theta_{19}$, we need to eliminate $d - 1$ of them from the likelihood function so that the latter becomes a function of θ_1 only. In general, it is extremely difficult to do this in a frequentist calculation in a way that preserves *exact* coverage over the entire parameter space. However, let $L_p(\theta_1) \equiv L(\theta_1, \hat{\theta}_2(\theta_1), \cdots)$ be the 1-dimensional *profile likelihood*, that is, the function obtained by maximizing the likelihood function $L(\theta_1, \theta_2, \cdots, \theta_{19})$ with respect to $\theta_2, \cdots, \theta_{19}$ for *fixed* θ_1 and replacing the exact, but unknown, values of $\theta_2, \cdots, \theta_{19}$ by their maximum likelihood estimates (MLE), $\hat{\theta}_2(\theta_1), \cdots, \hat{\theta}_{19}(\theta_1)$.

Replacing exact values by estimates is clearly an approximation. We should therefore not expect any procedure that uses this approximation to yield confidence limits and intervals with exact coverage. However, in practice, 1-dimensional profile likelihoods created from multi-parameter likelihood functions often perform surprisingly well [29]. Let L_{max} be the maximum of the likelihood function $L(\theta)$ and let $\Lambda = L_p/L_{max}$ be the likelihood ratio. If the partial derivatives with respect to θ_i of the likelihood function, $L(\theta)$, exist up to second order and they form a $d \times d$ non-singular matrix (the Hessian), the following result holds,

$$W = -2 \log \Lambda \rightarrow \chi^2, \tag{9}$$

as the amount of data grows without limit. This is Wilks theorem [28, 29]. For an approximate 95% C.L. lower limit on θ_1, we set $W = 1.64$, that is, $\Lambda = 0.44$, and solve for the lower limit.

Non-parametric profiling algorithm

The problem we need to solve is the following: for a fixed value of a parameter, say Q, we want to find the maximum value of the likelihood function when the latter is available only as a weighted swarm of points. The quantity Q could be a pMSSM parameter, a predicted observable of a sparticle mass. Here, written as pseudo-code, is our algorithm for finding the profile likelihood:

```
1 pMSSMPOINTS, QBIN, Q = inputs()
2 NBOOTSTRAP = 100
3 profile = 0

4 repeat NBOOTSTRAP times:

5       POINTS = generateBootstrapSample(pMSSMPOINTS)
6       histogram = histogramPoints(POINTS)

7       DMAX = -1
8       for point in POINTS:

9            if Q not in QBIN: continue

10            d = histogram.density(point)
11            if d > DMAX: DMAX = d

12       profile = profile + DMAX

13  profile = profile / NBOOTSTRAP
14  return profile
```

1 Get the pMSSM points, the bin $QBIN$ for which the profile likelihood is to be computed, and the value of Q.

6 Generate a d-dimensional histogram from current bootstrap sample.

9 Make sure Q lies in desired bin $QBIN$.

10,11 Find largest density $DMAX$ so far.

12–14 Return average of estimates of profile likelihood.

The above algorithm is implemented in a class we developed called `KDTProfileLikelihood`, which makes use of the multi-dimensional histogrammer `TKDTreeBinning` in Root. The d-dimensional histogram is created through recursive binary partitioning of the parameter space in such a way that bins have equal counts. The underlying data structure is a kd-tree [**?**].

Comparison of kinematic quantities with Full Simulation

We compare the important kinematic variables used for the study with the CMSSW Full simulation using LM1 benchmark point. Figures 15, 16, 17 shows that the simulation/reconstruction infrastructure used agree well with the full simulation.

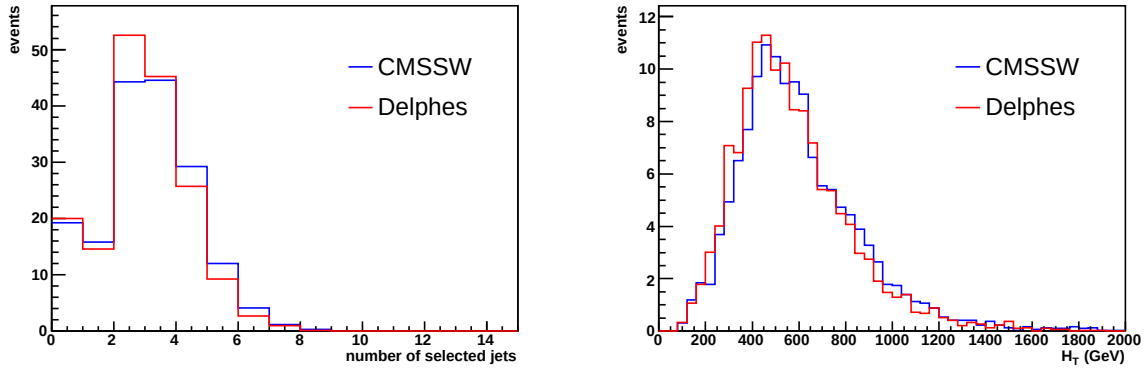

Figure 15: Event distribution using CMSSW Full simulation along with Delphes for LM1 benchmark points, as a function of jet multiplicity (left) and H_T (right)

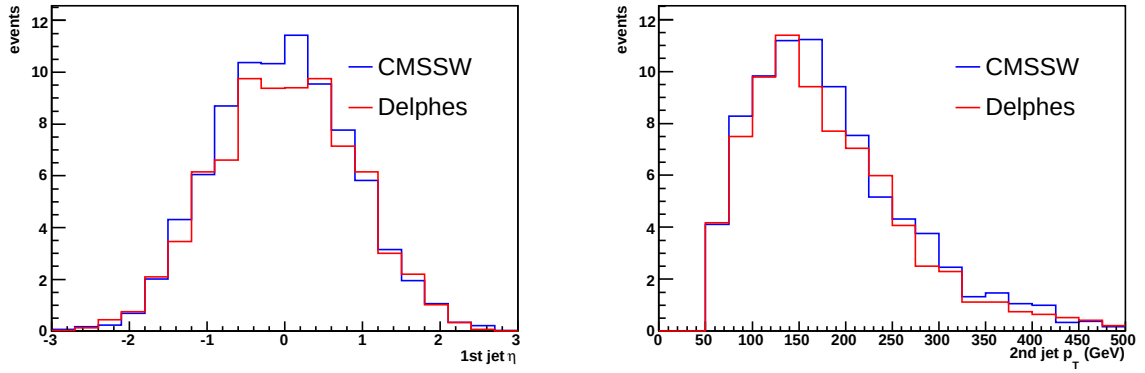

Figure 16: Event distribution using CMSSW Full simulation along with Delphes for LM1 benchmark points, as a function of pseudorapidity (left) and p_T of the jets (right)

References

[1] K. Choi and H. P. Nilles, JHEP **04**, 006 (2007), hep-ph/0702146.

[2] S. P. Martin, Phys. Rev. **D79**, 095019 (2009), 0903.3568.

[3] D. Horton and G. G. Ross, Nucl. Phys. **B830**, 221 (2010), 0908.0857.

[4] B. C. Allanach *et al.*, (2006), hep-ph/0602198.

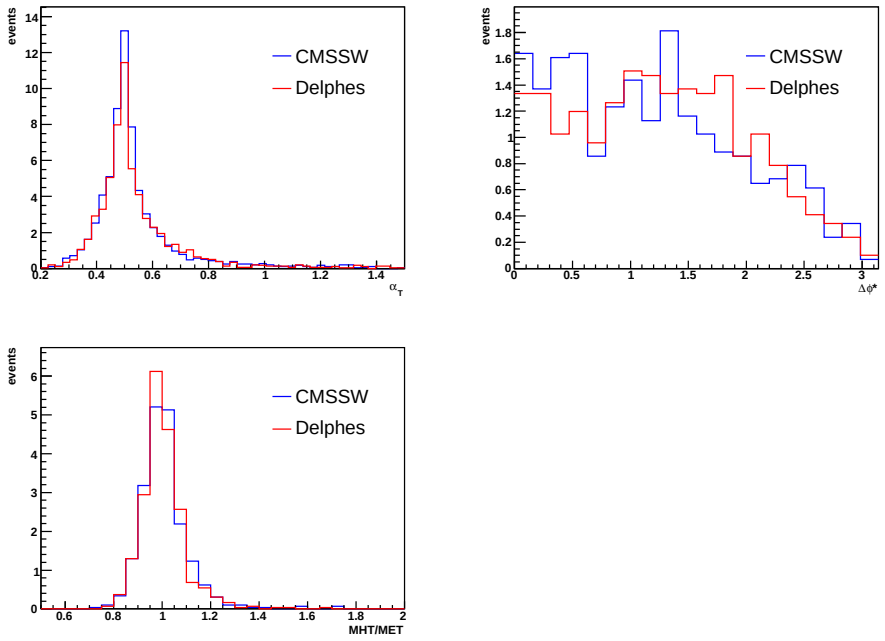

Figure 17: Event distribution using CMSSW Full simulation along with Delphes for LM1 benchmark points, as a function of α_T (top left), $\Delta\phi^*$ (top right) and MHT/MET (bottom)

[5] C. F. Kolda and S. P. Martin, Phys. Rev. **D53**, 3871 (1996), hep-ph/9503445.

[6] N. Polonsky and A. Pomarol, Phys. Rev. Lett. **73**, 2292 (1994), hep-ph/9406224.

[7] N. Polonsky and A. Pomarol, Phys. Rev. **D51**, 6532 (1995), hep-ph/9410231.

[8] J. R. Ellis, K. A. Olive, and Y. Santoso, Phys. Lett. **B539**, 107 (2002), hep-ph/0204192.

[9] C. F. Berger, J. S. Gainer, J. L. Hewett, and T. G. Rizzo, JHEP **02**, 023 (2009), 0812.0980.

[10] J. A. Conley, J. S. Gainer, J. L. Hewett, M. P. Le, and T. G. Rizzo, (2010), 1009.2539.

[11] L. Lyons, (ed.), R. P. Mount, (ed.), and R. Reitmeyer, (ed.), Prepared for PHYSTAT2003: Statistical Problems in Particle Physics, Astrophysics, and Cosmology, Menlo Park, California, 8-11 Sep 2003.

[12] Particle Data Group, K. Nakamura, J. Phys. **G37**, 075021 (2010).

[13] CDF and D0, and others, (2010), 1007.3178.

[14] ALEPH, DELPHI, L3 and OPAL collaborations and the LEP Working Group for Higgs Boson Searches, S. Schael *et al.*, Eur. Phys. J. **C47**, 547 (2006), hep-ex/0602042.

[15] G. Degrassi, S. Heinemeyer, W. Hollik, P. Slavich, and G. Weiglein, Eur. Phys. J. **C28**, 133 (2003), hep-ph/0212020.

[16] M. Davier, A. Hoecker, B. Malaescu, and Z. Zhang, (2010), 1010.4180.

[17] The Heavy Flavor Averaging Group, D. Asner *et al.*, (2010), 1010.1589.

[18] N. Jarosik *et al.*, (2010), 1001.4744.

[19] ALEPH, DELPHI, L3 and OPAL, LEP2 SUSY Working Group,, `http://lepsusy.web.cern.ch/lepsusy/`.

[20] P. Z. Skands *et al.*, JHEP **07**, 036 (2004), hep-ph/0311123.

[21] T. Sjostrand, S. Mrenna, and P. Z. Skands, JHEP **05**, 026 (2006), hep-ph/0603175.

[22] S. Ovyn, X. Rouby, and V. Lemaitre, (2009), 0903.2225.

[23] P. Z. Skands *et al.*, JHEP **0407** (2004) 036 [arXiv:hep-ph/0311123].

[24] T. Sjostrand, S. Mrenna and P. Z. Skands, JHEP **0605** (2006) 026 [arXiv:hep-ph/0603175].

[25] S. Ovyn, X. Rouby and V. Lemaitre, arXiv:0903.2225 [hep-ph].

[26] G. Belanger, F. Boudjema, A. Pukhov and A. Semenov, Comput. Phys. Commun. **176**, 367 (2007) [arXiv:hep-ph/0607059].

[27] F. Mahmoudi, Comput. Phys. Commun. **180**, 1579 (2009) [arXiv:0808.3144 [hep-ph]].

[28] S.S Wilks, "The large-sample distribution of the likelihood ratio for testing composite hypotheses," Ann. Math. Statist. **9**, 60-62 (1938).

[29] F. James, "Statistical Methods in Experimental Physics," 2nd Edition, (World Scientific, Singapore, 2008).

[30] CMS Collaboration, SUS-10-004 (in progress)